Power Multiplexing NOMA and Bandwidth Compression for Satellite-Terrestrial Networks

Min Jia, *Senior Member, IEEE*, Qiling Gao, Qing Guo, *Member, IEEE*, Xuemai Gu, *Member, IEEE*, and Xuemin Shen, *Fellow, IEEE*

***Abstract*—Due to the spectrum scarcity in the space information networks, non-orthogonal multiple access (NOMA) is envisioned as a promising technique in satellite-terrestrial communications networks as its improved system capacity and spectral efficiency. In this paper, to further improve the spectrum utilization efficiency in satellite-terrestrial networks, bandwidth compression (BC) design is embedded in the NOMA scheme, which contributes to the non-orthogonality both in power and frequency domains, named BC-NOMA. However, with such advantages provided by BC-NOMA, the inter-carrier interference (ICI) and the intra-group interference (IGI) are severe, which degrade the reliability and the capacity. Therefore, the impacts of BC and power domain multiplexing on the system capacity are first investigated. To cancel the mixed internal interference, an iterative and successive interference cancellation (ISIC) approach is proposed. Secondly, the symmetrical coding (SC) is designed with BC-NOMA to avoid the error propagation when using ISIC, which benefits much for the low power user (LUE). Furthermore, the closed-form expression of error probability for SCNOMA is derived and the system and individual capacities are also analyzed. Results show that the BC-NOMA system can achieve a quasi-optimal performance compared with the orthogonal subcarrier NOMA (ONOMA) system and balance the fairness.**

***Index Terms*—Bandwidth compression, BC-NOMA, ISIC, symmetrical coding, interference cancellation.**

I. Introduction

With the rapid development of wireless communications and the growth of the number of mobile devices, it is predicted that the mobile customers will reach to ten billion up to the 2020 [1]. As the global evolution of satellite-terrestrial networks, the conception of integration has been arisen these years, considering terrestrial networks to provide broadband services with low-cost and satellite networks to provide a complementary coverage for areas that cannot be covered by terrestrial networks [2]. Specifically, the quality of service (QoS) of cell-edge users can be enhanced significantly and the areas without terrestrial networks can be taken into account. Besides, spectrum sharing enabled satellite-terrestrial networks has been considered as a promising construct aiming at 5 G and beyond, and Internet of things (IoT) [3]–[5]. However, the increasing number of connections lead to the scarcity of spectrum resource, which expose an urgent requirement of higher communication efficiency with the expectation of serving a large amount of users.

To improve communication efficiency, the broadband spectrum sensing and the dynamic spectrum sharing techniques are proposed to address the spectrum scarcity problem [6], [7]. For the spectrum access, traditional orthogonal multiple access (OMA) and orthogonal frequency division multiple (OFDM) are leveraged to release the stress of spectrum [8]–[10], in both satellite and terrestrial networks. However, with the challenges of the large requirements of capacity and the shortage of spectrum, both satellite and terrestrial operators are trying to find a way to deal with the coming large amount of deployments [11]–[13].

To meet the aforementioned requirements, non-orthogonal techniques have attracted extensive attentions, such as non-orthogonal multiple access (NOMA) and spectrally efficient frequency division multiplexing (SEFDM) [11], [14]. It is well known that resource blocks in OMA, i.e., time slots or frequency subcarriers are segmented into orthogonal resource units and allocated to users independently [10], which means only one user is active at each time slot or each subcarrier [15]. In specific to power domain NOMA, multiple users share full time and frequency resources but multiplex power resource non-orthogonally at different levels [13], [14], [16], [17], which improves the efficiency of the physical resource utilization. For SEFDM, the subcarrier resources are packed with breaking orthogonality compared with OFDM [11], [18], which indicates that a certain amount of bandwidth resource can be saved for a given QoS constraint. Although such non-orthogonal techniques have been widely applied in 5 G networks and IoT networks [11], [13], it is still worth to point out that they have been investigated in satellite-terrestrial networks in recent years [2], [17], [18]. However, the inherent inter-carrier interference (ICI) and intra-group interference (IGI) of such spectrally efficient techniques bring great challenges to satellite-terrestrial networks.

In this paper, to benefit extremely from the limited spectrum resources of space information networks, the bandwidth compression NOMA (BC-NOMA) scheme for satellite-terrestrial networks is proposed, in which users access to the networks by

Manuscript received January 31, 2019; revised June 4, 2019 and August 16, 2019; accepted September 17, 2019. Date of publication September 26, 2019; date of current version November 12, 2019. This work was supported in part by the National Natural Science Foundation of China under Grants 61671183 and 61771163. The review of this article was coordinated by Prof. Igor Bisio. *(Corresponding author: Min Jia.)*

M. Jia, Q. Gao, Q. Guo, and X. Gu are with the Communication Research Center, School of Electronics and Information Engineering, Harbin Institute of Technology, Harbin, China (e-mail: jiamin@hit.edu.cn; 2456288241@qq.com; qguo@hit.edu.cn; guxuemai@hit.edu.cn).

X. Shen is with the Department of Electrical and Computer Engineering, University of Waterloo, 200 University Avenue West, Waterloo, On N2L3G1, Canada (e-mail: sshen@uwaterloo.ca).

Digital Object Identifier 10.1109/TVT.2019.2944077

power domain multiplexing and transmit information through non-orthogonal sub-carriers. Particularly, multiple users share full bandwidth resource and the bandwidth is sliced into non-orthogonal subcarriers. High system capacity and spectral efficiency can be achieved then. Main contributions of this paper are summarized as follows.

- The architectures of both uplink and downlink BC-NOMA scheme in satellite-terrestrial networks are constructed, the receiver design and signal detection scheme are given correspondingly. System capacity with BC-NOMA is investigated and the achievements of the throughout and the spectral efficiency are evaluated.
- The main challenge in BC-NOMA is to restrain the concomitant interference among multi-user and sub-carriers. We decompose the interference into two independent parts, which can be cancelled by the proposed ISIC detection algorithm. The quasi-optimal error performance can be achieved by ISIC and the user fairness is guaranteed.
- The symmetrical coding (SC) scheme aiming at the error performance optimization for the lower power user (LUE) is designed, which is distinguished from conventional NOMA structure. The error probability of SCNOMA is analyzed and the closed-form expression of error performance is given. The theoretical results show the enhanced performance of LUE through the utilization of SC, without additional influence upon HUE.
- Moreover, the BC-SCNOMA system is proposed. The association with bandwidth compression and symmetrical coding scheme benefit both the error performance of LUE and the system capacity. The bit-error-ratio (BER) performance is simulated with the utilization of ISIC and significant improvement can be further achieved.

The remainders of the paper are organized as follows. Related works are investigated following the introduction, in Section II. In Section III, the system model is demonstrated and the concerned problem is formulated. In Section IV, the capacity of BC-NOMA and error performance expressions are derived with the proposed detection method. In addition, theoretical and simulation results are shown in Section V. Finally, our conclusion is drawn in Section VI.

II. Related Works

Power domain multiplexing scheme has been utilized in satellite cluster networks as a hybrid method aiming at the improvement of spectrum opportunity [19], [20]. In [21]–[24], NOMA system is combined with multiple-input multiple-output (MIMO) system and the performance is evaluated. As a considerable hybrid up-down link design in satellite-terrestrial networks, a large magnitude of access subscribers are achieved in NOMA. Successive interference cancellation (SIC) method is usually applied within NOMA for signal detection and the performance of LUE is generally hard to guarantee [14], [25]. For the detection method of NOMA, many studies have been accomplished. The BER performance of downlink NOMA combined with OFDM is evaluated in visible light communication (VLC) systems [26], in which high order modulation is adopted. It reveals that it is hard to recover users' signals under traditional successive interference cancellation (SIC) method. In [19], the method of user pairing is formulated to get better cooperation performances. In [20] and [21], a power allocation algorithm towards user fairness is proposed according to the channel correlations between users and base stations (BSs). Some studies are done in UAV communications networks, i.e., an effective scheme was proposed to jointly optimize the trajectory of the UAV and the precoding of the BS in UAV-assisted NOMA networks [27]. It is known that the complexity of SIC depends on the times of subtraction, i.e., the number of multiplexing users in a group. Moreover, the proceeding error decision of the high power user (HUE) will cause the deterioration of the subsequent detection performance. To address the error propagation problem from the preceding level to the next one, a symmetrical coding method is used in visible light communication [28].

On the other hand, bandwidth compression scheme, i.e., SEFDM technique is raised to address the shortage of spectrum in satellite-terrestrial communications networks [11], [18]. Due to the shortage of the spectrum resources, the bandwidth compression scheme is put forward to improve the spectrum efficiency. In orthogonal multi-carrier systems, i.e., OFDM, the bandwidth is divided into multiple parallel orthogonal sub-carriers. However, with respect to BC scheme, non-orthogonal and over-lapping sub-carriers are employed to improve the spectrum utilization efficiency. The principle of BC is squeezing the sub-carriers closer with breaking the orthogonality and the interval between sub-carriers is adjusted by a compression factor [29]–[32]. Although the technique can improve the spectral efficiency up to 25% without performance degradation, the inherent ICI caused by non-orthogonal sub-carriers leads to terrible deterioration for BER performance and the detection complexity is increased [32], [33]. In [34], an iteration detector is proposed to achieve a lower complexity compared with the maximum likelihood (ML) detector. In [35], a newly fixed sphere decoder (FSD) and an improved FSD are investigated in order to solve the ICI problem more efficiently. Further, a detector based on quasi-orthogonality compensation (QOC) is proposed and an associative QOC-FSD detector is given for the performance improvement [11], [36]. However, such detectors are all limited to small system size.

III. System Model and Problem Formulation

A. Downlink Access in Satellite-Terrestrial Network Based BC-NOMA

The illustration of the downlink communications system in hybrid satellite-terrestrial networks is shown in Fig. 1, where the terrestrial communications system provides a high bandwidth and low-cost service for the terminals nearby BSs, and within the satellite coverage, the communication links are provided by satellite for the terminals at the edge of the service region. In other words, the satellite is regarded as the supplement to provide service for users beyond the service of BSs.

The total number of users in the coverage of satellite is defined as U_T, the number of BSs within the satellite coverage is L and the users served by the l^{th} BS are U_l. Thus, the

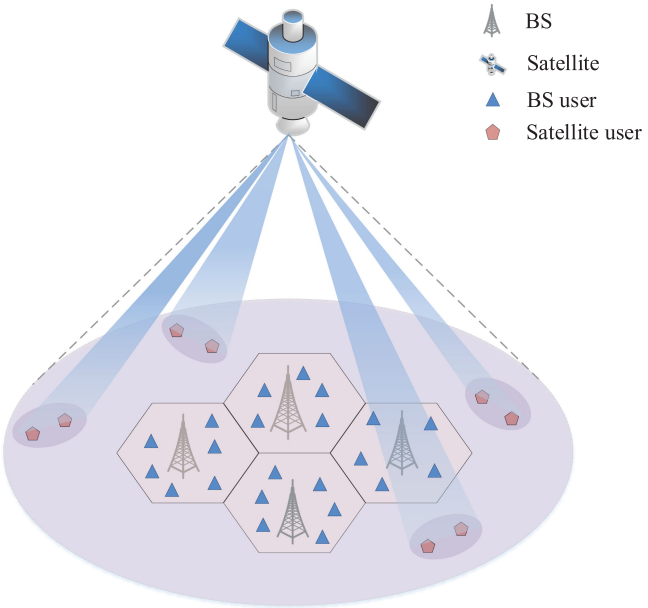

Fig. 1. Downlink access in hybrid satellite-terrestrial networks.

number of users only served by satellite can be expressed as $U_S = U_T - \sum_{l=1}^{L} U_l$. Note that no matter the terrestrial or the satellite users are arranged into multi-group under the utilization of NOMA. Especially for satellite terminals, the multi-beam technique is engaged to identify users in-ground, where the inter-beam interference is out of our work. We just consider the accessed terminals and the interference within a group.

The transmit signal of users in a group served by the l^{th} BS can be described as

$$S_l = \sum_{i=1}^{M_l} \sqrt{p_i} s_i, \tag{1}$$

where p_i is the power allocation coefficient of the i^{th} user, s_i is the modulated signal of the i^{th} user and M_l is the number of users within a group.

Considering users served by the satellite, similar to the terrestrial terminals, all users are divided into multi-group and only one group is taken into consideration. Thus, the signal transmitted by satellite is given as

$$S_s = \sum_{j=1}^{M_s} \sqrt{p_j} s_j, \tag{2}$$

where M_s denotes the satellite users within a group, p_j denotes the power allocated to the j^{th} user and s_j is the signal of the j^{th} user. Without loss of generality, the total transmit power is normalized, i.e., $\sum_{j=1}^{M_s} p_j = \sum_{i=1}^{M_g} p_{i,l} = 1$ and as well as the average symbol power, i.e., $E[|s_j|^2] = E[|s_{i,l}|^2] = 1$.

When applying NOMA in hybrid terrestrial-satellite networks, the interference environment is complicated, which contains not only the interference led by non-orthogonal access method but also the intra-group interference caused by multiple access. Taking all these interference into consideration, the

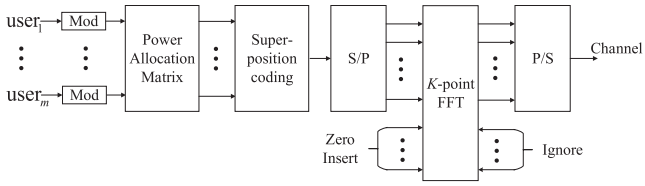

Fig. 2. Uplink model of BC-NOMA.

received signal at ξ is given as

$$y_\xi = h_\xi S_\xi + y_{or} + n, \tag{3}$$

where h_ξ is the channel state information between the transmitter and ξ, ξ stands for s and l, y_{or} is the interference from other groups, n denotes the additive white Gauss noise with σ^2 variance and zero mean. Further, y_{or} is expressed as

$$y_{or} = \sum h_{or} \sum_{v=1}^{M_{or}} \sqrt{p_v} s_v, \tag{4}$$

where h_{or} denotes the channel state information of the other groups within the coverage of BSs or the satellite, M_{or} is the number of grouped users.

Considering the technique we proposed in this paper, the properties of a single group are remarkable. Thus, the interference from other groups is neglected, only the intra-group interference is taken into consideration. The signal-to-interference-plus-noise (SINR) and system capacity are discussed in the following section.

B. Uplink and Downlink Model of BC-NOMA

The sententious model of uplink BC-NOMA is shown in Fig. 2, where non-orthogonal sub-carriers are used to transmit signals which are multiplexed in the power domain. Particularly, the signals of multi-user are modulated separately according to their modulation modes, then the modulated signals are superposed together under the premise of the power allocated to each user. K points IFFT is utilized to reflect the superposition signal into multi-carriers which are multiplexed in frequency domain with the employment of BC scheme. Specifically, the signals on multi-carriers are with all users' information, which means the frequency block is shared by all power domain multiplexing users.

According to the bandwidth compression scheme, power domain multiplexing signals are transmitted by sub-carriers which are non-orthogonal. In particular, the distance between adjacent sub-carriers is α times of that in OFDM with the limitation $0 < \alpha < 1$. The frequency distance between sub-carriers can be defined as $\Delta f = \frac{\alpha}{T}$, where T is the signal duration. After reflecting superposition signal into non-orthogonal multi-carrier, the normalized BC-NOMA signal is given as

$$x(t) = \frac{1}{\sqrt{T}} \sum_{k=-\infty}^{+\infty} \sum_{n=0}^{N-1} S_{k,n} \exp\left[\frac{j2\pi n\alpha(t-kT)}{T}\right], \tag{5}$$

where the number of sub-carriers is N, $S_{g,n}$ is the g^{th} superposition signal modulated on the n^{th} sub-carrier. After sampling,

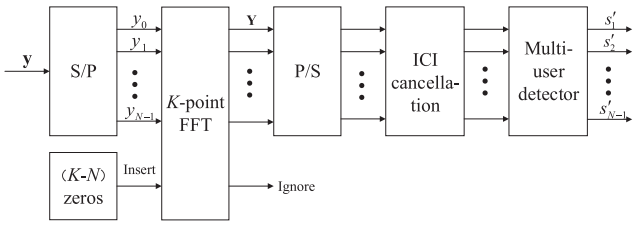

Fig. 3. Downlink model of BC-NOMA system.

(5) can be represented as

$$X[k] = \frac{1}{\sqrt{N}} \sum_{n=0}^{N-1} \left(\sum_{i=1}^{m} \sqrt{p_{i,k}} s_{i,k,n} \right) \exp\left(\frac{j2\pi nk\alpha}{N} \right). \quad (6)$$

Further, we reformulated (6) as the matrix format, by denoting $\mathbf{S}_N$ as the signal matrix with the information of all users, we have

$$\mathbf{X} = \mathbf{F}_K^{-1} \left([\mathbf{S}_N; \mathbf{0}_{K-N}] \right)$$
$$\mathbf{S}_N = \mathbf{ps}, \quad (7)$$

where $\mathbf{F}_K^{-1}$ denotes the K points IFFT matrix with elements equal to $e^{(\frac{j2\pi np\alpha}{N})}$, $\mathbf{p} = [p_1, p_2, \ldots, p_m]$ explains the power factor matrix allocated to users in a group. The matrix of multi-user is further expressed as

$$\mathbf{s} = \begin{bmatrix} s_{1,0} & s_{1,1} & \cdots & s_{1,N-1} \\ s_{2,0} & s_{2,1} & \cdots & s_{2,N-1} \\ \vdots & \vdots & \ddots & \vdots \\ s_{m,0} & s_{m,1} & \cdots & s_{m,N-1} \end{bmatrix}. \quad (8)$$

After discarding part of the data in $\mathbf{X}$, the final transmitted matrix is expressed as

$$\mathbf{X} = \Omega_N \left\{ \mathbf{F}_K^{-1} [\mathbf{ps}; \mathbf{0}_{K-N}] \right\}, \quad (9)$$

where $\Omega\{\cdot\}$ expresses the interception of the first N-dimension data.

As shown in Fig. 2, users in a group are multiplexed with different power and multi-user signals are transmitted through BC scheme. By employing the proposed scheme, the system capacity and spectral efficiency can be improved with the advantages provided by both power domain NOMA and BC schemes.

In Fig. 3, the model of downlink BC-NOMA is given. In particular, a K-points FFT is completed in the receiver corresponding to the K-points IFFT in the transmitter. The remaining part after FFT can be regarded as the superposition signal of multi-user. However, the mixed ICI and IGI are not tolerable. Thus, detectors have to be engaged in the receiver for the recovery of multi-user information.

According to the principle mentioned above, the received signal can be given as

$$y(t) = x(t) + n(t), \quad (10)$$

where $n(t)$ is the time domain white Gaussian noise with zero mean and σ^2 variance.

After Fast Fourier Transform (FFT) in the receiver, (10) is further expressed as

$$\mathbf{Y}' = \mathbf{CS} + \mathbf{N}, \quad (11)$$

where $\mathbf{S}$ is an N-dimensional vector of the transmitted signal, $\mathbf{C}$ is an $N \times N$ correlation matrix which is defined as $\mathbf{C} = \mathbf{F}_K^{-1}\mathbf{F}_K$, where $\mathbf{F}_K$ is the FFT matrix with elements equal to $e^{(\frac{-j2\pi nq\alpha}{N})}$. The element in the p^{th} row and the q^{th} column of matrix $\mathbf{C}$ is expressed as

$$c_{p,q} = \frac{1}{N} \sum_{n=0}^{N-1} \exp\left(\frac{j2\pi np\alpha}{N} \right) \exp\left(\frac{j2\pi nq\alpha}{N} \right)$$
$$= \begin{cases} 1, & p = q \\ \frac{1}{N} \frac{1-\exp(j2\pi\alpha(p-q))}{1-\exp\left(\frac{j2\pi\alpha(p-q)}{N}\right)}, & p \neq q, \end{cases} \quad (12)$$

where $p \neq q$, the elements in $\mathbf{C}$ are the interference between sub-carriers, which can be regarded as the intensity of ICI. In Fig. 3, corresponding to the IFFT in the transmitter, an FFT operation is done in the receiver and the received signal is given as

$$\mathbf{Y} = \Omega_N \left(\mathbf{C} \left(\sum_{i=1}^{m} \sqrt{p_{i,l}} s_{i,l,n} \right) + \mathbf{N} \right). \quad (13)$$

To restrain the maixed ICI and IGI caused by bandwidth compression and power domain multiplexing schemes, detection methods are appealed in downlink BC-NOMA to suppress the impacts of the non-orthogonal multi-carrier and recover the information of multi-user. Generally, SIC is utilized as a promising scheme for multi-user detection. However, to accommodate the mixed internal interference, the detection approach has to be updated and details are discussed in particular.

IV. Capacity and Proposed Detection for BC-NOMA

A. Network Capacity in BC-NOMA System

The capacity in BC-NOMA system is formulated in this part with the utilization of SIC, which means the first-decoded-user can be subtracted completely. In OFDM system, the total bandwidth is set as *B* and the number of co-channel is *M*. Thus, the frequency distance between adjacent sub-carriers can be expressed as

$$f = \frac{B}{MN}, \quad (14)$$

where N represents the number of sub-carriers in a co-channel.

Considering the BC scheme with a compression factor α, the frequency interval between the adjacent sub-carriers is

$$f_\alpha = \alpha f = \frac{\alpha B}{MN}. \quad (15)$$

Assuming the number of sub-carriers is defined as N. The data rate in the BC scheme is the same as in OFDM. The occupied bandwidth of the BC can be expressed as

$$B_\alpha = \frac{\alpha B}{M}. \quad (16)$$

It is obvious that for the same rate, the bandwidth compression scheme applies for less occupied bandwidth. And the total capacity of BC-NOMA system is given as

$$C = \sum_{i=1}^{m} \left(\sum_{k=1}^{K} B_\alpha \log_2 \left(1 + SINR_{k,i}\right) \right), \tag{17}$$

where $SINR_{k,i}$ is the SINR of the i^{th} user in the k^{th} co-channel, m is the number of users in a group and K is the number of co-channels.

In accordance of SIC, users with lower power are treated as interference, the capacity of the i^{th} user in the k^{th} co-channel is expressed as

$$C_{k,i} = \frac{\alpha B}{M} \log_2 \left(1 + \frac{p_{k,i} |h_{k,i}|^2}{\sum_{a=i+1} p_{k,a} |h_{k,i}|^2 + \sigma^2} \right), \tag{18}$$

where $p_{k,i}$ represents the power allocated to the i^{th} user in the k^{th} co-channel, $h_{k,i}$ is the channel state information and $|h_{k,i}|^2$ represents the k^{th} channel gain.

Following the principle of SIC, the multi-user detection is based on the sort of the power factors, each time for performing SIC, the information of HUE can be eliminated. Therefore, for the lowest power user, there is no interference from the other users and the capacity of the lowest power user is given as

$$C_{k,m} = B_k \log_2 \left(1 + \frac{p_{k,m} |h_{k,m}|^2}{\sigma^2} \right), \tag{19}$$

where $B_k = \frac{\alpha B}{M}$. Further,

$$p_{k,m} = \frac{\left(2^{\frac{C_{k,m}}{B_k}} - 1\right) \sigma^2}{|h_{k,m}|^2}. \tag{20}$$

where in (20), $R_{k,m} = \frac{C_{k,m}}{B_k}$ expresses the data rate. Considering the $(m-1)^{th}$ user next to the lowest one, it is easy to find that

$$\begin{aligned} C_{k,m-1} &= B_k \log_2 \left(1 + \frac{p_{k,m-1} |h_{k,m-1}|^2}{p_{k,m} |h_{k,m}|^2 + \sigma^2} \right) \\ &= B_k \log_2 \left(1 + \frac{p_{k,m-1} |h_{k,m-1}|^2}{\sigma^2 2^{R_{k,m}}} \right). \end{aligned} \tag{21}$$

Further, (21) can be reformulated as

$$p_{k,m-1} |h_{k,m-1}|^2 = 2^{R_{k,m}} \sigma^2 (2^{R_{k,m-1}} - 1). \tag{22}$$

Specifically, the derivation can be applied to the arbitrary user in the group and the capacity of the i^{th} user in the group is expressed as

$$C_{k,i} = \frac{\alpha B}{M} \log_2 \left(1 + \frac{p_{k,i} |h_{k,i}|^2}{\sigma^2 2^{\sum_{a=i+1}^{m} \frac{MC_{k,a}}{\alpha B}}} \right). \tag{23}$$

Observing that the user with the lowest power determines the capacity of the BC-NOMA system. Compared with orthogonal frequency and orthogonal multiple access (O-OMA) system, for the same transmission bandwidth, the number of accessed users in BC-NOMA system has increased $\frac{m}{\alpha}$ times, where m is the number of users within a group and α represents the compression factor in BC scheme.

B. Performance of the Proposed Detection Algorithm

1) ISIC Algorithm: In the receiver, the performance deterioration caused by the mixed interference is severe, for the proposed detection algorithm, the IGI and ICI are considered simultaneously. In this part, an ISIC algorithm is proposed to restrain ICI and recover multi-user information from the superposition signal. The main idea of ISIC is defined as

$$\mathbf{y} = \lambda \mathbf{R} + (\mathbf{e} - \lambda \mathbf{C}) \mathbf{S}_{z-1}, \tag{24}$$

where $\mathbf{R}$ is the received signal, $\mathbf{S}_{z-1}$ is an N-dimensional vector of the estimated signal after the z^{th} iteration, $\mathbf{e}$ is an identity matrix, λ is the convergence factor and $\mathbf{y}$ is the final estimated signal, which can be regarded as the superposition signal of multi-user. In the receiver, the ICI and IGI are deemed as independent parts. After performing (24), the remaining part in the l^{th} group is expressed as

$$\mathbf{y} = \mathbf{h}_l{}^{\mathrm{T}} \mathbf{p} \mathbf{s}^{\mathrm{T}} + \mathbf{n}_l, \tag{25}$$

where the variables in (25) can be further expressed as

$$\mathbf{h}_l = [h_{l,1}, h_{l,2}, \cdots, h_{l,m}]^{\mathrm{T}}, \tag{26}$$

$$\mathbf{n}_l = [n_{l,1}, n_{l,2}, \cdots, n_{l,m}]^{\mathrm{T}}. \tag{27}$$

Thus, (25) can be represented as

$$\mathbf{y} = \begin{bmatrix} y_{l,1} = h_{l,1} \sum_{i=1}^{m} \sqrt{p_{l,i}} s_{l,i} + n_{l,1} \\ y_{l,2} = h_{l,2} \sum_{i=1}^{m} \sqrt{p_{l,i}} s_{l,i} + n_{l,2} \\ \cdots \\ y_{l,m} = h_{l,m} \sum_{i=1}^{m} \sqrt{p_{l,i}} s_{l,i} + n_{l,m} \end{bmatrix}. \tag{28}$$

Notice that the power allocation principle in NOMA is correlated to the channel gains, users with better channel conditions are equipped with lower power factors and users far from BS are with higher power factors. Obviously, for the user with the worst channel condition, there is no need to perform SIC, the desired signal can be decoded for the first time.

Details of ISIC algorithm are given in Algorithm 1, where $\hat{\mathbf{S}}$ is the expression of the unconstrained estimated symbols and $\mathbf{S}'$ is the N-dimensional vector of the constrained estimated symbols. λ is the convergence factor limited as $1 \leq \lambda \leq 2$, v is the number of iterations and z represents the z^{th} iteration.

We further discuss the complexity of the proposed ISIC compared with the conventional ML detector. The received signal is given as (11) and the process of ML detector can be represented as $\tilde{\mathbf{s}}_1 = \arg\min_{\mathbf{s} \in Z^m} \|\mathbf{Y} - \mathbf{C}\mathbf{s}\|^2$, where $\tilde{\mathbf{s}}_1$ is the estimated signal and $\mathbf{s}$ is the ergodic exact constellations vector. Thus, the complexity of ML is defined as

$$t_M = 2N^2 Z^{Nm} + 2N^2 \cong O(2N^2 Z^{Nm}). \tag{29}$$

The complexity of ISIC is regarded as the summation of two parts and given as

$$t_I = 4mZN^3 v + 2(m-1)N^2 v, \tag{30}$$

Algorithm 1: Iteration Successive Interference Cancellation (ISIC) Algorithm.

Input: $\mathbf{R}, \mathbf{C}, v, \lambda$, certain region $C_d^{\Re_i}$ of constellation $\Re_i$, $\Re_i \in \mathbf{R}$
Output: user signal $\mathbf{s}_1, \mathbf{s}_2$;
$\mathbf{S}' = \mathbf{R}$;
$z = 1$;
while $z \leq v$ **do**
  $\hat{\mathbf{S}} = \lambda\mathbf{R} + (\mathbf{e} - \lambda\mathbf{C})\,\mathbf{S}'$;
  $d = \sqrt{p_2}\,(1 - z/v)$;
  mapping signal $\hat{\mathbf{S}}$;
  if $\hat{\mathbf{S}} \in C_d^{\Re_i}$ **then**
    $\mathbf{S}'_i = \Re_i$;
  else
    $\mathbf{S}'_i = \hat{\mathbf{S}}$;
    end;
  $z = z + 1$;
  $\mathbf{y} = \hat{\mathbf{S}}$;
  $\mathbf{s_2} = \mathrm{demo}\,(\mathbf{y})$;
  $\mathbf{s_1} = \mathbf{y} - \mathrm{mod}\,(\mathbf{s_2})$;
  end;
Procedure End

where Z is the number of constellations defined by modulation mode, m is the number of users within a group, N is the number of subcarriers and v is the iteration times in ISIC.

2) Symmetrical Coding Based on NOMA: In downlink NOMA, distance users decode their data directly and users with better channel conditions need to perform SIC to recover their signals. Aiming at the terminals have to perform SIC, users with high power are decoded first and then the desired signal can be recovered through subtraction.

Extra interference is produced as a result of the preceding detection errors. Generally, the users closed to BS are asserted to get a preferable performance, while in conventional NOMA, users with better channel conditions are allocated with lower power factors which cause inferior performance.

In this part, an algorithm engaged in NOMA is arisen for the sake of the error reatraints. The construction of SCNOMA is given with the dereferencing operators κ_1 and κ_2, the values of κ_1 and κ_2 are closely related to HUE. Through completing symmetrical coding before superposition coding and anti-symmetrical coding (ASC) after SIC, the error delivery can be restrained mostly. Details of SC and ASC are shown in the algorithm tables below.

As shown in Algorithm 2, the signal after SC is expressed as

$$\mathbf{a} = \mathbf{p}\mathbf{M}^T, \tag{31}$$

where $\mathbf{p}$ is the power factor matrix with elements equal to $\sqrt{p_i}$, $i = 1, 2, \ldots, m$ and $\mathbf{M}^T$ expresses the traverse matrix. Signals after SC are superposed and then transmitted. Thus, the ASC has to be performed in the receiver after SIC corresponding to the transmitter. Details of ASC are given in Algorithm 3. In next part, the closed BER expressions are derived with the utilization of SCNOMA, which demonstrate the benefits in theoretical.

Algorithm 2: SCNOMA Algorithm.

Input: user signal $\mathbf{s}$,power matrix $\mathbf{p}$
Output: superposition signal $\mathbf{S}$
sorted as $\mathbf{p} = [p_{min}, \cdots, p_m]$;
$\mathbf{s} = [\mathbf{s}_1, \cdots, \mathbf{s}_m]$;
$\mathbf{S} = \mathbf{s}_1$;
$i = 1$;
while $i \leq m$ **do**
  if $l \leq \mathrm{length}\,(\mathbf{s}_{i+1})$ **then**
    $\kappa_1 = (-1)^{\left\lceil \frac{1}{2} - \frac{\mathrm{real}(s_{i+1,l})}{2\left|\mathrm{real}(s_{i+1,l})\right|} \right\rceil}$;
    $\kappa_2 = (-1)^{\left\lceil \frac{1}{2} - \frac{\mathrm{imag}(s_{i+1,l})}{2\left|\mathrm{imag}(s_{i+1,l})\right|} \right\rceil}$;
    $l = l + 1$;
  else
    end;
  foreach i **do**
    $S_l = s_{i+1,l} + \kappa_1 real(S_l) + j\kappa_2 imag(S_l)$;
    $i = i + 1$;
  end;
Procedure End

Algorithm 3: Anti-Symmetrical Coding basd NOMA (ASC-NOMA) Algorithm.

Input: received signal $\mathbf{S}$
Output: multi-user $\mathbf{s}$
$i = 1$;
$l = 1$;
$\mathbf{s}_m = \mathrm{demo}\,(\mathbf{S})$;
while $i \leq m - 1$ **do**
  $\hat{\mathbf{s}}_{m-i} = \mathrm{demo}\left(\mathbf{S} - \sum_{a=0}^{i-1} \hat{\mathbf{s}}_{m-a}\right)$;
  $i = i + 1$;
  if $l \leq \mathrm{length}\,(\hat{\mathbf{s}}_{m-i})$ **then**
    $\kappa_1 = (-1)^{\left\lceil \frac{1}{2} - \frac{\mathrm{real}(s_{m-i-1,l})}{2\left|\mathrm{real}(s_{m-i-1,l})\right|} \right\rceil}$;
    $\kappa_2 = (-1)^{\left\lceil \frac{1}{2} - \frac{\mathrm{imag}(s_{m-i-1})}{2\left|\mathrm{imag}(s_{m-i-1})\right|} \right\rceil}$;
    $s_{m-i,l} = \kappa_1 \mathrm{real}\,(\hat{s}_{m-i,l}) + \kappa_2 \mathrm{imag}\,(\hat{s}_{m-i,l})$;
    $l = l + 1$;
  else
    end;
  end;
Procedure End

C. BER Performance Analysis of SCNOMA

1) BER Performance of HUE: According to the signal model presented in (1) and Algorithm 2, only a single group is taken into consideration and the number of users within a group is set as 2. Signal after SC and superposition coding is defined as

$$S = \sum_{i=1}^{2} \sqrt{p_i}\hat{s}_i + n, \tag{32}$$

where p_1 and p_2 are the power factors with the limitation $p_1 + p_2 = 1,\ p_1 > p_2$, $\hat{s}_i$ is the signal of the i^{th} user after the symmetrical coding and the transmit power is normalized. For the simplicity, the modulation mode is selected as BPSK in both HUE and LUE. Without loss of generality, any modulation modes, i.e., QAM, can be employed. Note that distance between constellations has to be updated corresponding to the modulation mode [37].

Retrospecting to the principle of the symmetrical coding scheme, it adds no effect on HUE, which means no additional gain is acquired on the performance of HUE compared with conventional NOMA. We assume that all modulated symbols have equal priori probability and the error probability of HUE can be defined as

$$p_e^{HUE} = p\left(s_1 = 1\right) p\left(h_1 S + n < 0 \,|s_1 = 1\right) + p\left(s_1 = 0\right) p\left(h_1 S + n > 0 \,|s_1 = 0\right). \tag{33}$$

To avoid long expressions inside the formula, the probability events $s_1 = 1$ and $s_1 = 0$ are represented as ξ_1 and ξ_2. Then the error probability in (33) can be rewritten as

$$p\left(\xi_1\right) = p\left(s_1 s_2 = [1,0]\right) + p\left(s_1 s_2 = [1,1]\right), \tag{34}$$

$$p\left(\xi_1\right) = p\left(s_1 s_2 = [1,0]\right) + p\left(s_1 s_2 = [1,1]\right), \tag{35}$$

After superposition coding, the error probability can be defined as

$$\begin{aligned} p_e^{HUE} = {} & p\left(\xi_1\right) p\left(n \geq \sqrt{p_1} h_1 + \sqrt{p_2} h_1 \,|\xi_1\right) \\ & + p\left(\xi_1\right) p\left(n \leq -\sqrt{p_1} h_1 - \sqrt{p_2} h_1 \,|\xi_1\right) \\ & + p\left(\xi_2\right) p\left(n \geq \sqrt{p_1} h_1 - \sqrt{p_2} h_1 \,|\xi_2\right) \\ & + p\left(\xi_2\right) p\left(n \geq -\sqrt{p_1} h_1 + \sqrt{p_2} h_1 \,|\xi_2\right). \end{aligned} \tag{36}$$

The probability of an A event under the condition of B event is

$$P\left(A\,|B\right) = \frac{P(AB)}{p(B)}. \tag{37}$$

Thus, (36) can be further formulated as

$$\begin{aligned} p_e^{HUE} = {} & \frac{1}{2}\left\{p\left(n \geq \sqrt{p_1} h_1 + \sqrt{p_2} h_1\right)\right. \\ & \left. + p\left(n \geq \sqrt{p_1} h_1 - \sqrt{p_2} h_1\right)\right\}, \end{aligned} \tag{38}$$

further, we have

$$\begin{aligned} p_e^{HUE} = {} & \frac{1}{2} Q\left(\frac{\sqrt{p_1} h_1 + \sqrt{p_2} h_1}{\sigma}\right) \\ & + \frac{1}{2} Q\left(\frac{\sqrt{p_1} h_1 - \sqrt{p_2} h_1}{\sigma}\right). \end{aligned} \tag{39}$$

The expressions inside $Q(\cdot)$ in (39) are reperesented as

$$\begin{aligned} \upsilon_1^2 &= \frac{\left(\sqrt{p_1} + \sqrt{p_2}\right)^2 E\left[|h_1|^2\right]}{\sigma^2}, \\ \upsilon_2^2 &= \frac{\left(\sqrt{p_1} - \sqrt{p_2}\right)^2 E\left[|h_1|^2\right]}{\sigma^2}, \end{aligned} \tag{40}$$

where the expectation operator of the channel state information is limited as $E[|h_i|^2] = 1,\ i = 1, 2$. Notably, υ_1^2 and υ_2^2 denote the SINR after superposition coding, which means the SINR of the superposition signal is the only determinant of the error performance. Further, substituting (40) into (39), the error probability of HUE is given as

$$p_e^{HUE} = \frac{1}{2}\left[Q\left(\upsilon_1\right) + Q\left(\upsilon_2\right)\right], \tag{41}$$

2) BER Performance of LUE: Based on the sequence of detection, it is obvious that the error of the first-decode-user derives additional interference to the next one. Thus, the total error performance of LUE is the summation of two parts: the error caused by the erroneous detection of HUE and the error caused by self detection.

$$p_e^{LUE} = p_1^{LUE} + p_2^{LUE}, \tag{42}$$

where for the sake of the simplicity, we define $p_1^{LUE} = p\left(\text{correct}_{HUE}\right) p(\text{error}_{LUE}|\text{correct}_{\text{HUE}})$ as the error probability caused by self detection and $p_2^{LUE} = p(\text{error}_{HUE}) p\left(\text{error}_{LUE}|\text{error}_{HUE}\right)$ as the delivery from HUE to LUE.

In Algorithm 2, after subtracting the signal of HUE, the remaining signal is given as

$$y_2 = \begin{cases} h_2 \kappa \sqrt{\alpha_2} x_2 + n, & (a) \\ h_2\left(2\sqrt{\alpha_1} x_1 + \kappa \sqrt{\alpha_2} x_2\right) + n, & (\mathrm{b}) \end{cases} \tag{43}$$

where in (43), formula (a) expresses the signal after a successful SIC and (b) expresses the signal after an unsuccessful SIC. Definition of κ is given in Algorithm 2, where the value of κ is relevant to the real and the imagine parts of HUE.

Similar to the derivation of HUE, the error probability of LUE caused by previous erroneous detection is given as

$$\begin{aligned} p_2^{LUE} = {} & \frac{1}{2} p\left(n \geq 2\sqrt{p_1} h_2 - \sqrt{p_2} h_2\right) \\ & + \frac{1}{2} p\left(\sqrt{p_1} h_2 + \sqrt{p_2} h_2 \leq n \leq 2\sqrt{p_1} h_2 + \sqrt{p_2} h_2\right), \end{aligned} \tag{44}$$

the same as (44), the error caused by self detection can be derived as

$$\begin{aligned} p_1^{LUE} = {} & \frac{1}{2} p\left(n \leq -\sqrt{p_2} h_2\right) \\ & + \frac{1}{2} p\left(\sqrt{p_2} h_2 \leq n \leq \left(\sqrt{p_1} + \sqrt{p_2}\right) h_2\right). \end{aligned} \tag{45}$$

Further, we make some replacements as

$$\begin{aligned} \upsilon_3^2 &= \frac{\left(2\sqrt{p_1} - \sqrt{p_2}\right)^2}{\sigma^2} E\left[|h_2|^2\right], \\ \upsilon_4^2 &= \frac{\left(\sqrt{p_1} + \sqrt{p_2}\right)^2}{\sigma^2} E\left[|h_2|^2\right], \\ \upsilon_5^2 &= \frac{\left(2\sqrt{p_1} + \sqrt{p_2}\right)^2}{\sigma^2} E\left[|h_2|^2\right], \end{aligned} \tag{46}$$

the final expression of p_2^{LUE} can be rewritten as

$$p_2^{LUE} = \frac{1}{2}\left[Q\left(\upsilon_3\right) + Q\left(\upsilon_4\right) - Q\left(\upsilon_5\right)\right]. \tag{47}$$

TABLE I
SIMULATION PARAMETERS

Parameter	Value
Compression factor α	$\frac{7}{8}$
The number of subcarriers K	8
Dominant power allocation factor p_1	Fixed (0.7, 0.75, 0.8)
Non-dominant power allocation factor p_2	Fixed (0.3, 0.25, 0.2)
Iteration times v	1000
Convergence factor λ	1.1
Monte Carlo Simulation repeated times	10^6
Transmit power of BS	1(Normalized)
Channel state	AWGN
Modulation mode	BPSK
The number of users m	2 (Extensible)

Similarly, we define $v_6^2 = \frac{p_2}{\sigma^2} E[|h_2|^2]$. Hence, the error probability of p_1^{LUE} can be represented as

$$p_1^{LUE} = \frac{1}{2}\{Q(v_6) + [Q(v_6) - Q(v_4)]\}$$
$$= Q(v_6) - \frac{1}{2}Q(v_4). \quad (48)$$

Substituting (47) and (48) into (42), the total error probability of LUE is

$$p_e^{LUE} = \frac{1}{2}[2Q(v_6) + Q(v_3) - Q(v_5)]. \quad (49)$$

In conventional NOMA scheme, the error probability of LUE caused by self detection is expressed as $p_\ell = \frac{1}{2}[-Q(v_1) + 2Q(v_6)]$. Based on the properties of Q function, there achieves $p_e^{LUE} \cong p_\ell$.

V. SIMULATION RESULTS AND DISCUSSIONS

In this section, numerical results are provided to facilitate the performance evaluation of the proposed scheme and the detection algorithm in satellite-terrestrial networks. Monte Carlo Simulations are conducted and simulation results are proposed to verify the analysis results. Simulation parameters without particular definition are given in Table I.

The comparisons of accessed users in O-OMA, bandwidth compression and orthogonal multiple access system (BC-OMA) and BC-NOMA system are shown in Fig. 4. For the same transmission bandwidth, the BC-OMA scheme can achieve a larger user number compared with the O-OMA system. Similarly, through multiplexing in power domain, A larger quantity of accessed users has been achieved in the BC-NOMA system. Simulation results indicate that the BC-NOMA scheme can achieve a prominent increase contrasted to the O-OMA and the BC-OMA systems.

Fig. 5 gives the illustration of the user capacity according to (23). Based on the proceeding work, the system capacity is relevant to the capacity of the lowest power user. Simulation shows the capacity curves of HUE and LUE versus the compression factor and the power allocation factor, note that the decrease of

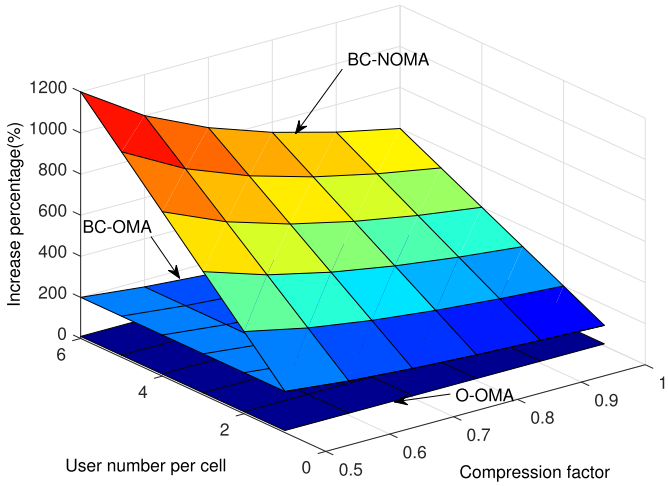

Fig. 4. Increase percentage in O-OMA, BC-OMA and BC-NOMA systems.

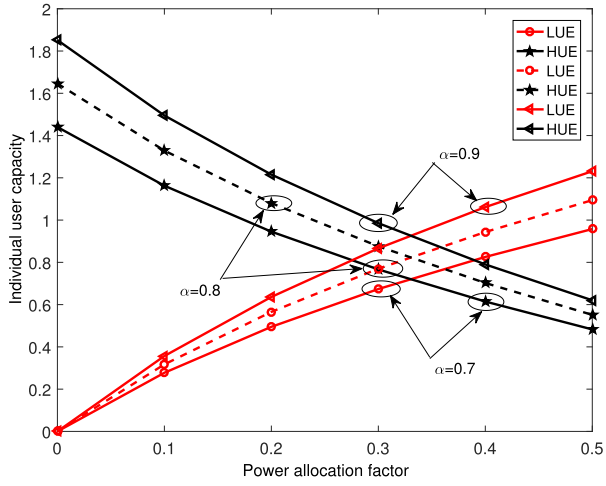

Fig. 5. User capacity based on BC-NOMA.

the compression factor α means the decrease of the occupied bandwidth.

Observe from Fig. 6, p_e^{LUE} achieves an approximate performance compared with the performance without error delivery in conventional NOMA. Specifically, the higher SNR value exhibits a better approximate performance, which indicates the interruption of the error delivery.

Fig. 7 illustrates the BER comparisons of the symmetrical coding scheme and conventional SIC, the results are compared between SNR = 5 dB and SNR = 10 dB versus the power factor p_1. It can be observed that the SC scheme aids to achieve a better performance in a certain range of p_1, when p_1 falls out of the range, it is clear that SIC performs an alight advantage.

In Fig. 8, the BER performances of SCNOMA versus SNR are given according to (41) and (49). Results under simulation and analysis are given below. It is obvious that the proposed SC-NOMA scheme has a positive effect on the error performance of LUE. Especially, with the increasing power allocated to LUE, the error performance of LUE is getting better while deterioration has occurred on the performance of HUE.

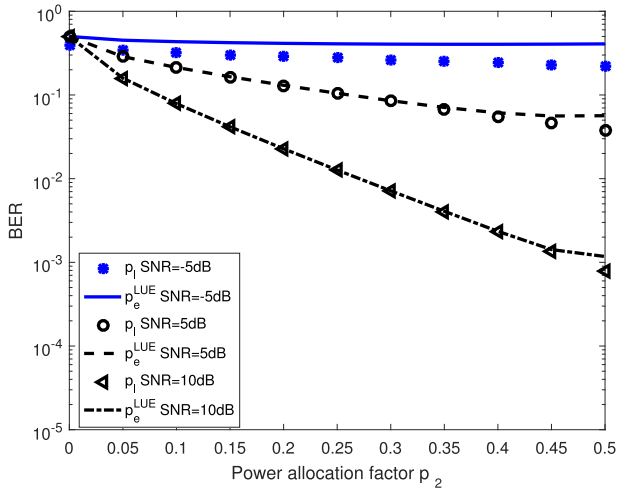

Fig. 6. p_ℓ and p_e^{LUE} comparisons with different power allocation factor p_2.

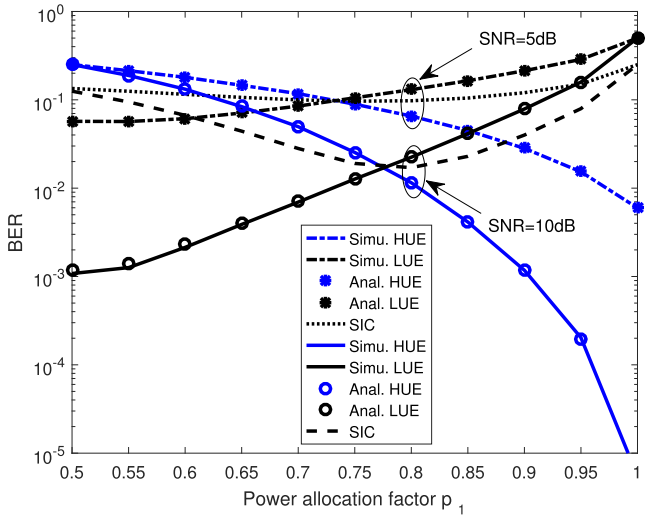

Fig. 7. BER comparisons with different power allocation factor p_1.

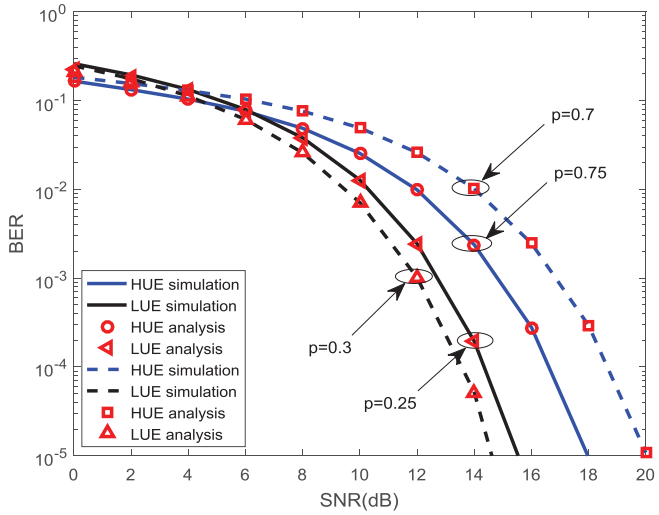

Fig. 8. BER performance of downlink symmetrical coding NOMA.

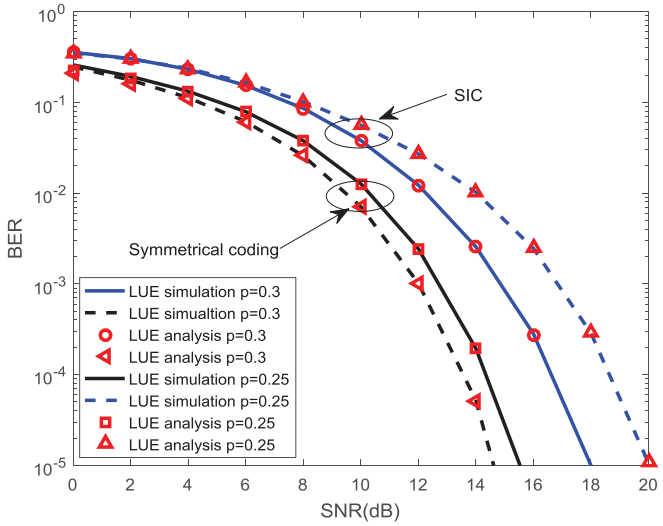

Fig. 9. BER performance of LUE under symmetrical coding and conventional SIC.

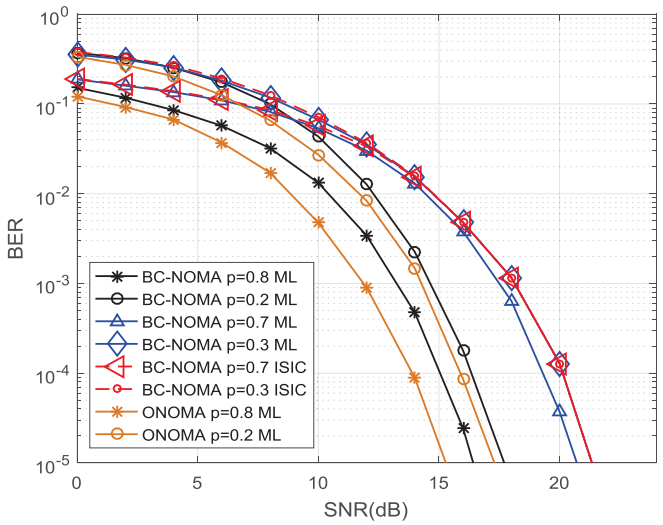

Fig. 10. BER performance in BC-NOMA and ONOMA system.

Fig. 9 demonstrates the BER performance comparisons of LUE between downlink NOMA based on the symmetrical coding and conventional SIC. Both simulation and analysis results are given. In accordance with analysis, simulation results indicate the benefits of the upon LUE with the utilization of SC. Compared with the SIC scheme, less SNR is required in the SCNOMA scheme for the same magnitude of error performance.

In the preceding work, the analysis and simulation results under the symmetrical coding are given and the positive effects on the error performance are indicated. Further, the symmetrical coding scheme is engaged in the proposed BC-NOMA system to achieve an enhanced performance. In the following simulations, the comparisons between ISIC and ML are given, performances under BC-SCNOMA and conventional NOMA are given simultaneously.

Fig. 10 shows the simulation results of the error performance in ONOMA and BC-NOMA systems. ML and ISIC algorithms

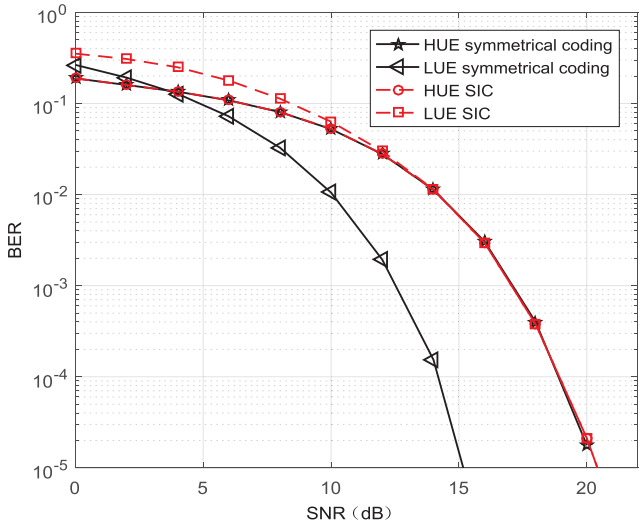

Fig. 11. BER performance of symmetrical coding in BC-NOMA system.

are employed and the performances are simulated jointly. The SNR required in BC-NOMA is 3 dB larger than ($\mathrm{BER} = 10^{-5}$) in ONOMA system when an approximate error performance is achieved. Further, in SC embedded BC-NOMA system, the BER comparisons of ISIC and ML algorithms are simulated jointly. Observe from the results, an approximate performance is achieved with the utilization of ISIC compared with ML algorithm. However, in preceding work, the complexity of ISIC and ML is derived, which indicates that the proposed ISIC algorithm requires fewer operations, especially when the number of sub-carriers has reached to a certain level. Moreover, effects on the power allocation factors are evaluated and discussed. The approximate power factors between users can cause a more rigorous IGI, which further leads to the performance deterioration.

Fig. 11 shows the BER comparisons in BC-SCNOMA and BC-NOMA systems. Observe that for the same BER performance of LUE, a quite less SNR is demanded with the utilization of the symmetrical coding and the performance of HUE with and without SC are identical. Simulation results indicate that with the utilization of SC in BC-NOMA system, an enhanced performance can be achieved without any deterioration on HUE. Specifically, the performance requirements can be achieved for the user sacrificing more power in the NOMA system. In our summation, through the uniting of the bandwidth compression scheme and NOMA, together with the proposed detection methods, a predictable benefit can be achieved.

VI. Conclusion

In this paper, BC-NOMA system has been investigated in hybrid satellite-terrestrial networks, bandwidth compression scheme is engaged in conventional NOMA for the improvement of the system capacity and spectral efficiency. First, system models of uplink and downlink BC-NOMA in satellite-terrestrial networks are given and predictable benefits are evaluated. Second, a corresponding detector is proposed to restrain the impacts of the concomitant interference, i.e., ICI and IGI which are caused by bandwidth compression and power domain multiplexing. With the proposed ISIC algorithm, the mixed interference can be mostly remitted, moreover, the SC scheme is engaged in the proposed scheme for an additional benefit on BER performance. Third, the interference between users in satellite-terrestrial networks has been formulated, individual and system capacity in the proposed BC-NOMA system are given, closed BER expression under the symmetrical coding scheme has been formulated and the benefits to LUE have been identified in theory simultaneously. Simulation and analysis results indicate that BC-NOMA system has achieved a larger accessed user number and the error probability of ISIC has achieved an approximate performance compared with ML. Conclusively, the BC-NOMA scheme aims to the improvement of spectral efficiency and the proposed algorithms are advantageous to the interference cancellation and performance enhancement.

References

[1] X. Zhu, C. Jiang, L. Yin, L. Kuang, N. Ge, and J. Lu, "Cooperative multigroup multicast transmission in integrated terrestrial-satellite networks," *IEEE J. Sel. Areas Commun.*, vol. 36, no. 5, pp. 981–992, May 2018.

[2] X. Zhu, C. Jiang, L. Kuang, N. Ge, and J. Lu, "Non-orthogonal multiple access based integrated terrestrial-satellite networks," *IEEE J. Sel. Areas Commun.*, vol. 35, no. 10, pp. 2253–2267, Oct. 2017.

[3] M. Jia, X. Gu, Q. Guo, W. Xiang, and N. Zhang, "Broadband hybrid satellite-terrestrial communication systems based on cognitive radio toward 5G," *IEEE Wireless Commun.*, vol. 23, no. 6, pp. 96–106, Dec. 2016.

[4] M. Jia, X. Liu, X. Gu, and Q. Guo, "Joint cooperative spectrum sensing and channel selection optimization for satellite communication systems based on cognitive radio," *Int. J. Satellite Commun. Netw.*, vol. 35, no. 2, pp. 139–150, Dec. 2017.

[5] X. Zhang *et al.*, "Distributed compressive sensing augmented wideband spectrum sharing for cognitive IoT," *IEEE Internet Things J.*, vol. 5, no. 4, pp. 3234–3245, Aug. 2018.

[6] Y. Ma, Y. Gao, Y. Liang, and S. Cui, "Reliable and efficient sub-nyquist wideband spectrum sensing in cooperative cognitive radio networks," *IEEE J. Sel. Areas Commun.*, vol. 34, no. 10, pp. 2750–2762, Oct. 2016.

[7] Z. Qin, Y. Gao, M. D. Plumbley, and C. G. Parini, "Wideband spectrum sensing on real-time signals at sub-nyquist sampling rates in single and cooperative multiple nodes," *IEEE Trans. Signal Process.*, vol. 64, no. 12, pp. 3106–3117, Jun. 2016.

[8] A. H. Khan, M. A. Imran, and B. G. Evans, "Semi-adaptive beamforming for OFDM based hybrid terrestrial-satellite mobile system," *IEEE Trans. Wireless Commun.*, vol. 11, no. 10, pp. 3424–3433, Oct. 2012.

[9] B. F. Beidas and R. Iyer Seshadri, "OFDM-like signaling for broadband satellite applications: Analysis and advanced compensation," *IEEE Trans. Commun.*, vol. 65, no. 10, pp. 4433–4445, Oct. 2017.

[10] A. Leith, M.-S. Alouini, D. I. Kim, X. Shen, and Z. Wu, "Flexible proportional-rate scheduling for OFDMA system," *IEEE Trans. Mobile Comput.*, vol. 12, no. 10, pp. 1907–1919, Oct. 2013.

[11] M. Jia, Z. Yin, Q. Guo, G. Liu, and X. Gu, "Downlink design for spectrum efficient IoT network," *IEEE Internet Things J.*, vol. 5, no. 5, pp. 3397–3404, Oct. 2018.

[12] E. Altubaishi and X. Shen, "Performance analysis of spectrally efficient amplify-and-forward opportunistic relaying scheme for adaptive cooperative wireless systems," *Wireless Commun. Mobile Comput.*, vol. 15, no. 8, pp. 1247–1258, Aug. 2015.

[13] S. M. R. Islam, N. Avazov, O. A. Dobre, and K. Kwak, "Power-domain non-orthogonal multiple access (noma) in 5G systems: Potentials and challenges," *IEEE Commun. Surveys Tut.*, vol. 19, no. 2, pp. 721–742, Apr. 2017.

[14] Z. Ding, Z. Yang, P. Fan, and H. V. Poor, "On the performance of non-orthogonal multiple access in 5G systems with randomly deployed users," *IEEE Signal Process. Lett.*, vol. 21, no. 12, pp. 1501–1505, Dec. 2014.

[15] K. Janghel and S. Prakriya, "Performance of adaptive OMA/cooperative-NOMA scheme with user selection," *IEEE Commun. Lett.*, vol. 22, no. 10, pp. 2092–2095, Oct. 2018.

[16] X. Yan, H. Xiao, K. An, G. Zheng, and W. Tao, "Hybrid satellite terrestrial relay networks with cooperative non-orthogonal multiple access," *IEEE Commun. Lett.*, vol. 22, no. 5, pp. 978–981, May 2018.

[17] X. Shao, Z. Sun, M. Yang, S. Gu, and Q. Guo, "NOMA-based irregular repetition slotted aloha for satellite networks," *IEEE Commun. Lett.*, vol. 23, no. 4, pp. 624–627, Apr. 2019.

[18] H. Ghannam and I. Darwazeh, "SEFDM over satellite systems with advanced interference cancellation," *IET Commun.*, vol. 12, no. 1, pp. 59–66, Jan. 2018.
[19] M. Jia, X. Liu, Z. Yin, Q. Guo, and X. Gu, "Joint cooperative spectrum sensing and spectrum opportunity for satellite cluster communication networks," *Ad Hoc Netw.*, vol. 58, pp. 231–238, 2017. [Online]. Available: http://www.sciencedirect.com/science/article/pii/S1570870516301342
[20] N. Zhao *et al.*, "Joint beamforming and jamming optimization for secure transmission in MISO-NOMA networks," *IEEE Trans. Commun.*, vol. 67, no. 3, pp. 2294–2305, Mar. 2019.
[21] Y. Chi, L. Liu, G. Song, C. Yuen, Y. L. Guan, and Y. Li, "Practical MIMO-NOMA: Low complexity and capacity-approaching solution," *IEEE Trans. Wireless Commun.*, vol. 17, no. 9, pp. 6251–6264, Sep. 2018.
[22] L. Liu, C. Yuen, Y. L. Guan, Y. Li, and C. Huang, "Gaussian message passing for overloaded massive MIMO-NOMA," *IEEE Trans. Wireless Commun.*, vol. 18, no. 1, pp. 210–226, Jan. 2019.
[23] Z. Ding, R. Schober, and H. V. Poor, "A general MIMO framework for NOMA downlink and uplink transmission based on signal alignment," *IEEE Trans. Wireless Commun.*, vol. 15, no. 6, pp. 4438–4454, Jun. 2016.
[24] Z. Ding, F. Adachi, and H. V. Poor, "The application of MIMO to non-orthogonal multiple access," *IEEE Trans. Wireless Commun.*, vol. 15, no. 1, pp. 537–552, Jan. 2016.
[25] G. Im and J. H. Lee, "Outage probability for cooperative NOMA systems with imperfect SIC in cognitive radio networks," *IEEE Commun. Lett.*, vol. 23, no. 4, pp. 692–695, Apr. 2019.
[26] H. Ren *et al.*, "Performance improvement of M-QAM OFDM-NOMA visible light communication systems," in *Proc. IEEE Global Commun. Conf.*, Dec. 2018, pp. 1–5.
[27] N. Zhao, X. Pang, Z. Li, Y. Chen, F. Li, Z. Ding, and M.-S. Alouini, "Joint trajectory and precoding optimization for UAV-assisted NOMA networks," *IEEE Trans. Commun.*, vol. 67, no. 5, pp. 3723–3735, May 2019.
[28] H. Li, Z. Huang, Y. Xiao, S. Zhan, and Y. Ji, "Solution for error propagation in a NOMA-based VLC network: Symmetric superposition coding," *Opt. Exp.*, vol. 25, pp. 29856–29863, Nov. 2017.
[29] D. Nopchinda, T. Xu, R. Maher, B. C. Thomsen, and I. Darwazeh, "Dual polarization coherent optical spectrally efficient frequency division multiplexing," *IEEE Photon. Technol. Lett.*, vol. 28, no. 1, pp. 83–86, Jan. 2016.
[30] T. Xu and I. Darwazeh, "Transmission experiment of bandwidth compressed carrier aggregation in a realistic fading channel," *IEEE Trans. Veh. Technol.*, vol. 66, no. 5, pp. 4087–4097, May 2017.
[31] I. Darwazeh, T. Xu, T. Gui, Y. Bao, and Z. Li, "Optical SEFDM system; bandwidth saving using non-orthogonal sub-carriers," *IEEE Photon. Technol. Lett.*, vol. 26, no. 4, pp. 352–355, Feb. 2014.
[32] S. V. Zavjalov, S. V. Volvenko, and S. B. Makarov, "A method for increasing the spectral and energy efficiency SEFDM signals," *IEEE Commun. Lett.*, vol. 20, no. 12, pp. 2382–2385, Dec. 2016.
[33] T. Xu and I. Darwazeh, "A soft detector for spectrally efficient systems with non-orthogonal overlapped sub-carriers," *IEEE Commun. Lett.*, vol. 18, no. 10, pp. 1847–1850, Oct. 2014.
[34] S. Isam, I. Kanaras, and I. Darwazeh, "A truncated SVD approach for fixed complexity spectrally efficient fdm receivers," in *Proc. IEEE Wireless Commun. and Netw. Conf.*, Mar. 2011, pp. 1584–1589.
[35] T. Xu, R. C. Grammenos, F. Marvasti, and I. Darwazeh, "An improved fixed sphere decoder employing soft decision for the detection of non-orthogonal signals," *IEEE Commun. Lett.*, vol. 17, no. 10, pp. 1964–1967, Oct. 2013.
[36] M. Jia, Z. Yin, Q. Guo, and X. Gu, "Compensation of non-orthogonal ICI for SEFDM receivers," in *Proc. IEEE/CIC Int. Conf. Commun. China*, Oct. 2017, pp. 1–5.
[37] F. Kara and H. Kaya, "BER performances of downlink and uplink NOMA in the presence of SIC errors over fading channels," *IET Commun.*, vol. 12, no. 15, pp. 1834–1844, Sep. 2018.

Min Jia (M'13–SM'17) received the Ph.D. degree from Sung kyung kwan University, Seoul, South Korea, and the Harbin Institute of Technology, Harbin, China, in 2010. She is currently an Associate Professor and a Ph.D. Supervisor with the Communication Research Center, School of Electronics and Information Engineering, Harbin Institute of Technology. Her current research interests include cognitive radio, digital signal processing, machine learning, and broadband satellite communications.

Qiling Gao received the B.Eng. degrees in information and communication engineering from Harbin Engineering University, Harbin, China, in 2018. She is currently working toward the Ph.D. degree with the School of Electronics and Information Engineering, Harbin Institute of Technology. Her research interests include nonorthogonal multiple access and resource allocation.

Qing Guo (M'11) received the M.Eng. and Ph.D. degrees in information and communication engineering from the Harbin Institute of Technology, Harbin, China, in 1990 and 1998, respectively. He is currently a Professor and the Dean with the School of Electronics and Information Engineering, Harbin Institute of Technology. His research interests include satellite communications, deep space communications, wireless transmissions, and broadband multimedia communication techniques.

Xuemai Gu received the M.Sc. and Ph.D degrees from the Harbin Institute of Technology, Harbin, China, in 1985 and 1991, respectively. He is currently a Professor with the Graduate School, Harbin Institute of Technology. His research interests include integrated and hybrid satellite and terrestrial communications and broadband multimedia communication technique.

Xuemin (Sherman) Shen (M'97–SM'02–F'09) received the Ph.D. degree in electrical engineering from Rutgers University, New Brunswick, NJ, USA, in 1990. He is currently a University Professor with the Department of Electrical and Computer Engineering, University of Waterloo, Waterloo, ON, Canada. His research focuses on resource management in interconnected wireless/wired networks, wireless network security, social networks, smart grids, and vehicular ad hoc and sensor networks. Dr. Shen is a registered Professional Engineer of Ontario, Canada, an Engineering Institute of Canada Fellow, a Canadian Academy of Engineering Fellow, a Royal Society of Canada Fellow, and a Distinguished Lecturer of the IEEE Vehicular Technology Society and Communications Society. He has received the Excellent Graduate Supervision Award, in 2006, and the Outstanding Performance Award five times from the University of Waterloo and the Premier's Research Excellence Award (PREA), in 2003, from the Province of Ontario, Canada. He received the R.A. Fessenden Award in 2019 from IEEE, Canada, the James Evans Avant Garde Award in 2018 from the IEEE Vehicular Technology Society, the Joseph LoCicero Award in 2015 and the Education Award in 2017 from the IEEE Communications Society. He served as the Technical Program Committee Chair/Co-Chair for the IEEE Global Communications Conference (Globecom) 2016, the IEEE International Conference on Computer Communications (Infocom) 2014, the IEEE Vehicular Technology Conference (VTC) 2010 Fall, the IEEE Globecom 2007, the Symposia Chair for the IEEE International Conference on Communications (ICC) 2010, the Tutorial Chair for the IEEE VTC 2011 Spring, the Chair for the IEEE Communications Society Technical Committee on Wireless Communications, and P2P Communications and Networking. He is the Editor-in-Chief of the IEEE Internet of Things Journal and the Vice President on Publications of the IEEE Communications Society.